Thermodynamic stability at phase coexistence

Jozismar Rodrigues Alves [*] and Vera Bohomoletz Henriques [†]

Instituto de Física, Universidade de São Paulo, Rua do Matão, 1371, CEP: 05508-090, São Paulo, SP, Brasil

The main point we address in this paper is the question of thermodynamic stability for phase-separating systems, at coexistence in equilibrium. It has long been known that numerical simulations of different statistical models may yield "Van der Waals-like" isotherms in the coexistence region. Such "inverted" convexity segments of thermodynamic fields, known as unstable, are forbidden by the second law of thermodynamics on entropy, and their presence is not justified in exact results. In numerical experiments, their origin has been associated with the interface between the two coexisting phases. Nonetheless, the violation of the second law by entropy has not yet, to our knowledge, been rationalized. In this work, we introduce the thermodynamics of the interface between coexisting phases and give an alternative interpretation to the theory developed by Hill in the 1960s. Our approach points to a misinterpretation of the usual measurements of thermodynamic potentials in simulations. Correct interpretation eliminates the unstable regions of the true potentials. Our adapted theory is verified for the 2D lattice gas through carefully planned simulations. The thermodynamic description of the interface behavior inside the coexistence region restores the proper convexity of the true chemical potential isotherms. As a bonus, our interpretation allows direct calculation of surface tension in very good accordance with Onsager's analytic prediction.

I. INTRODUCTION

The 19th-century experimental study of coexisting gas-liquid phases [1] showed that the system pressure-volume isotherms present a horizontal plateau which signals the presence of phase separation. The first successful theory for Andrews data [1] was proposed by Van der Waals [2]: it had the advantage of presenting two different densities for the same pressure, at fixed lower temperatures, as observed for the liquid-gas coexistence isotherms. However, instead of the plateau between the liquid and gas volumes, the pressure vs volume isotherm presented a small concave segment at intermediary volumes, with inversion of convexity. This feature was corrected by Maxwell, who proposed the insertion by hand of a coexistence plateau (following experimental results) which linked the gas and liquid convex branches [3, p. 163]. Van der Waals's and equivalent mean-field approaches gained widespread applications, which are extremely useful in the areas of condensed and soft matter to this day.

The 20th century brought about investigation of models for fluids through computer simulations. Differently from the analytical results for mean-field models, numerical experiments of statistical models were able to present gas-liquid coexistence. Surprisingly, the coexistence region was characterized by inverted convexity segments in field-density isotherms [4–9]. This feature, change of convexity, violated a fundamental property of entropy. This should not be expected from the exact treatment of statistical models. Clarification of this question is the aim of this paper.

Thermodynamic variables have well-defined convexity properties [10, p. 206], [11, p. 682], [12, p. 74], [13, p. 37], [14], all of which derive from the second law of thermodynamics. In equilibrium, entropy $S(U, V, N)$ is a concave function of its extensive variables (internal energy U, volume V, or particle number N, in the case of a simple fluid), which is a consequence of the fact that entropy must be a maximum at the equilibrium of composite systems, with respect to possible partitions of extensive variables in an isolated system. Thus, we must have $\partial^2 S/\partial X^2 < 0$, where X denotes an extensive variable. This property of entropy propagates to the thermodynamic potentials obtained through Legendre transformation, such as the Helmholtz free energy, $F(T, V, N)$, which is a convex function of volume V ($\partial^2 F/\partial V^2 > 0$), for instance. An inversion of convexity violates the second law of thermodynamics. A negative $\partial^2 F/\partial V^2$ implies expansion under increasing pressure, which explains why an inversion in convexity also comes under the name of thermodynamic instability ([10, Ch. 8] and [12, p. 76]).

If thermodynamics is obtained from the statistical mechanics of a given model, the derived potentials must have the proper convexity as prescribed by the second law. Calculations for the average properties of the model may be developed in different ensembles, the choice of which is usually guided by mathematical simplicity. Ensembles may be classified into two different categories (see Sec. III of [15]): *density*, or an extensive variables ensemble, for which densities such as energy, volume, particle number, or magnetization are fixed; or in the corresponding conjugate *field* ensembles, at fixed temperature, pressure, chemical potential, or magnetic field, to cite the more common ensembles. It is in the density ensembles that the convexity problem is known to arise [4–9].
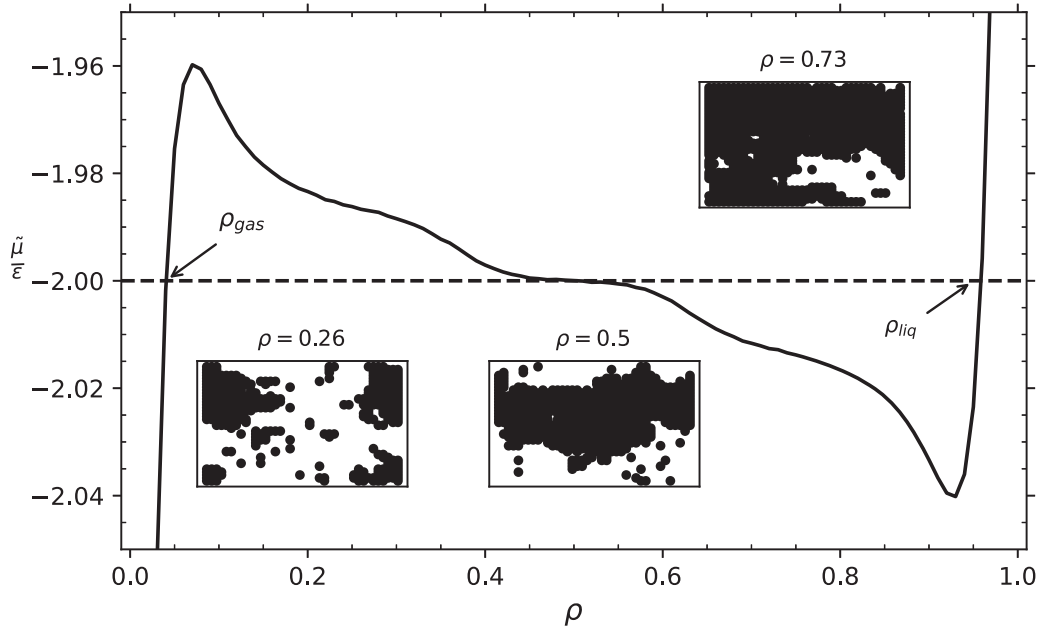
---
[*]jozismar.alves@alumni.usp.br
[†]verahenriques@usp.br

FIG. 1. Lattice gas chemical potential μ vs density ρ isotherm below criticality obtained from MC simulations in the (T, V, N) canonical ensemble. Insets correspond to the periodic system snapshots at three different densities: $\rho = 0.26$ in the left loop, $\rho = 0.5$ in the middle of the plateau region, and $\rho = 0.73$ in the right loop. The dashed line is an extension of the plateau region, and its intersections with the isotherm correspond to the phase coexistence densities. Data are for $L = 40$ and reduced temperature $t = 0.5$ (see Sec. III for variable definitions).

In order to address the problem of thermodynamic instability, which is systematically associated with phase separation, we shall adopt the term *loop* for the segment of inverted convexity which arises in the isotherms of different field thermodynamic variables, as functions of their conjugate densities (see [12, p. 76]).

Violation of convexity properties, or loops, thus seem to arise under two very different treatments of statistical models: (1) in mean-field approaches [3,10], as in the case of the well-known Van der Waals concave "loops" in pressure vs volume isotherms, which present segments with negative compressibility, i.e., $(\partial V/\partial P)_{T,N} = -[\partial^2 F/\partial V^2]_{T,N}^{-1} < 0$, or (2) in *numerical simulations* at fixed density ensembles [4–7], which may yield "loops" in chemical potential μ as a function of density $[(\partial \mu/\partial N)_{T,V} = (\partial^2 F/\partial N^2)_{T,V} > 0]$, as illustrated in Fig. 1, or of temperature as a function of energy $[(\partial T/\partial E)_{V,N} = -T^2(\partial^2 S/\partial E^2)_{V,N} > 0]$ [8,9].

In both cases, mean-field analytical treatment, or numerical simulations, the region of forbidden convexity presents itself in association with coexistence of thermodynamic phases of the model systems. However, the rationale behind the loops, which may arise in the two situations mentioned above, have completely different origins, as has been pointed out elsewhere [7].

The cause of the nonphysical or forbidden loops in the thermodynamics of mean-field models is well established as an artifact of the calculations, which assume the system to be homogeneous throughout the coexistence region [3, p. 41]. Since Maxwell, the forbidden loops are substituted *ad hoc* with a coexistence plateau which connects the two single phase branches, accepted as correct for the model system. This is the well-known "Maxwell construction," also known as "equal area construction,"

a reference to the mathematical property yielded by the procedure [3, p. 163].

In the case of numerical simulations of statistical models, the origin of the forbidden *loops* must be looked for elsewhere. Differently from the mean-field approaches, numerical experiments in fixed extensive variable ensembles, such as microcanonical [8] or canonical ensembles [4–7,16,17], allow for the appearance of different coexisting phases. If one fixes an intermediate density, between the gas and liquid densities, for example, the numerical system necessarily partitions into a gas and a liquid phase if temperature is sufficiently low. It is exactly in these density ensembles, in which different phases develop simultaneously, that thermodynamic instability, or loops, appear. However, this situation is totally different from the situation of Van der Waals-like systems, which are treated as homogeneous throughout. Thus loops must have a different explanation for the case of simulations.

Several studies have attributed chemical potential loops obtained in canonical ensemble simulations to interface effects in finite systems, which should disappear in the thermodynamic limit [17]. The de-escalating of loops with size has been indicated very clearly in several numerical studies [7,16]. Characteristics of special loop segments have also been closely associated with interface geometry [7]. However, violation of convexity remained without an explanation.

In this study, we focus on the convexity inversion in chemical potential isotherms which arise in simulations in the canonical ensemble (see Fig. 1). We argue that these loops are only apparent, and disappear under correct thermodynamic analysis of phase coexistence.

The grand-canonical fixed chemical potential ensemble presents a different picture: the system remains homogeneous throughout the simulations, even under coexistence or near

coexistence conditions, but alternates between the two phases. Instead of loops one sees a region of apparent metastability which is reminiscent of magnetic hysteresis, with the low-density phase presenting itself beyond the coexistence potential, as it is increased, whereas the high-density phase remains present below the coexistence chemical potential, as the latter is decreased [18].

In summary, numerical simulations of phase-separating systems in the coexistence region seem to yield both thermodynamic instability, through the presence of loops in thermodynamic variables, as well as the nonequivalence of ensembles: "loops" in density ensembles, or hysteresis in field ensembles, for the same thermodynamic field variable. Both features have been reputed to be a consequence of the finiteness of the simulated systems [6,18].

In this paper we address the following question: what could be the origin of the apparent thermodynamic instability seen in simulations for thermodynamic fields such as chemical potential? Is instability justified in finite systems?

We recover a theory proposed by Hill [17] for the thermostatistics of different ensembles of systems at coexistence, presented by the author at the dawn of numerical investigation of statistical model properties. We add an alternative interpretation to Hill's approach by introducing the thermodynamics of the interface between coexisting phases, which had not been included in his theory. The ensemble probability distributions are corrected correspondingly. Proper treatment of the thermodynamics of the interface yields the recovery of proper thermodynamic stability, as we show in Sec. II. This is the main point of our work.

In order to illustrate and prove our point of view, we explore the behavior of statistics in both the canonical and grand-canonical ensembles, and obtain the corresponding thermodynamics, for the case of the square lattice gas model. By applying the thermodynamics of the interface in the interpretation of results, thermodynamic stability of the chemical potential is regained, as shown in Sec. III A.

Additionally, two side products of our investigation of convexity were obtained. Our adaptation of Hill's theory requires that we couple the investigations in both ensembles: the grand-canonical and the canonical ensemble. The apparent divergence between canonical and grand-canonical results disappears, as very low probability spatial configurations are probed in the fixed field ensemble. As well, as a consequence of our approach we also obtain a straightforward method for measuring the interface tension between two coexisting phases from numerical experiments, which is much simpler than existing methods (see, for example, [7]). The latter is presented in Sec. III B.

II. THERMOSTATISTICS OF PHASE COEXISTENCE

What is the precise origin of loops in numerical simulations? In the 1960s Hill [17] presented a theory aimed at answering this question, which we describe briefly. Let Y represent a thermodynamic field and X the respective conjugate density. At a particular density X, a system at coexistence presents two different densities, say, X_1 and X_2, which represent the densities of the two coexisting phases. If one runs simulations for fixed conjugate field Y, density X fluctuates

around the two values X_1 and X_2. Thus, if one plots the probability $P(X; Y)$ of density X at fixed thermodynamic field Y, one obtains a two-peak function, with peaks centered on X_1 and X_2, separated by a minimum at X_{min}.

For clarity of argument, let us consider a simple fluid. The grand-canonical probability of finding N particles in the system at (T, V, μ) is given by

$$P(N; T, V, \mu) = \frac{e^{\beta \mu N} Z(T, V, N)}{\Xi(T, V, \mu)}, \quad (1)$$

where $Z(T, V, N)$ and $\Xi(T, V, \mu)$ are, respectively, the canonical and the grand canonical partition functions of the system, and $\beta = 1/k_B T$.

According to Hill's proposal, the maximum of the distribution $[\frac{\partial P(N; T, V, \mu)}{\partial N}]_{T,V,\mu} = 0$ should yield the chemical potential in the canonical ensemble:

$$\beta \mu + \frac{1}{Z(T, V, N)} \frac{\partial Z(T, V, N)}{\partial N} = 0 \quad (2)$$

in accordance with the corresponding equation of state in the Helmholtz free-energy representation

$$\left(\frac{\partial F}{\partial N} \right)_{T,V} = \mu(T, V, N). \quad (3)$$

According to Hill [17], the liquid-gas coexistence would be signaled by a two-peaked distribution of particle number N for the system in the chemical potential bath, thus yielding two maximum values for particle density, corresponding to N_{gas} and N_{liq}, at the same chemical potential μ_{cx}.

However, as we will show below, Eq. (3) is correct only for the homogeneous phases. In the coexistence region, the system free energy must include dependence on the behavior of the interface between coexisting phases: Eq. (3) is no longer valid, and Hill's theory must be modified accordingly.

The full expression for the free energy of a simple fluid at coexistence, F_{cx}, must be written as

$$F_{cx}(T, V, N) = F_{bulk} + F_{int}(T, V, N), \quad (4)$$

where $F_{bulk} = F_{gas}(T, V_{gas}, N_{gas}) + F_{liq}(T, V_{liq}, N_{liq})$. Note that $N = N_{gas} + N_{liq}$ and $V = V_{gas} + V_{liq}$. The free energy of the interface is given by

$$F_{int} = \gamma(T) A_{int}(T, V, N), \quad (5)$$

where γ describes surface tension, while A_{int} is the area of the interface [19,20].

From Eqs. (4) and (5), a new equation of state related to variation of the number of particles is obtained:

$$\left(\frac{\partial F_{cx}}{\partial N} \right)_{T,V} = \mu_{cx}(T, V, N) + \gamma \left(\frac{\partial A_{int}}{\partial N} \right)_{T,V}, \quad (6)$$

where the coexistence chemical potential is obtained from the bulk free energies as

$$\mu_{cx}(T, V, N) = \left(\frac{\partial F_{bulk}}{\partial N} \right)_{T,V}. \quad (7)$$

Equation (7) results from equality of the chemical potentials of the different phases under equilibrium,

$$\mu_{cx} = \left(\frac{\partial F_{gas}}{\partial N_{gas}} \right)_{T,V} = \left(\frac{\partial F_{liq}}{\partial N_{liq}} \right)_{T,V}, \quad (8)$$

and from $N_{gas} + N_{liq} = N$.

At coexistence, Eq. (6) replaces the usual state equation for the chemical potential [Eq. (3)]. This is the main point of our work, with important consequences on the interpretation of simulation results, as we show in the next section.

It will be useful to define a pseudochemical potential $\tilde{\mu}$, related to the true coexistence chemical potential μ_{cx} through

$$\tilde{\mu}(T, V, N) = \mu_{cx}(T, V, N) + \gamma \left(\frac{\partial A_{int}}{\partial N} \right)_{T,V}. \tag{9}$$

Note that Eq. (6) implies that in order to obtain the true chemical potential from the system free-energy behavior under variation of particle number one should maintain interface area fixed. Thus it is clear that, at coexistence, computing the usual partial derivative of the system free energy [Eq. (3)] with respect to particle number, at fixed temperature and volume, does *not* yield the chemical potential but, instead, the sum of the chemical potential with a term proportional to the variation of the interface area with particle number [Eq. (6)].

Interpretation of Eq. (9) is as follows: free-energy variation with particle number, at coexistence, must yield the plateau (given by μ_{coex}), expected at phase separation, plus a term which describes the rate of variation of the interface with particle number. This rate is positive when the interface is forming, and is negative in the region in which the interface is disappearing. As we shall discuss in the following section, this additional term is responsible for the loops which appear in the pseudochemical potential we have defined, while the true chemical potential displays the correct plateau behavior.

What about the grand-canonical ensemble probability $P(N; T, V, \mu)$? If the usual grand-canonical probability is written in terms of the true chemical potential of the homogeneous phase [Eq. (1)], at coexistence the probability distribution for the number of particles [Eq. (1)] must be rewritten in order to include the interface area effect. Thus one must write

$$P(N; T, V, \tilde{\mu}) = \frac{e^{\beta \tilde{\mu} N} Z(T, V, N)}{\Xi(T, V, \tilde{\mu})}. \tag{10}$$

The interface contribution is represented through $\tilde{\mu}$.

Under the circumstances of coexistence, extrema with respect to particle number N of the the distribution function at coexistence $P(N; T, V, \tilde{\mu})$ are given by

$$\beta \tilde{\mu} + \frac{1}{Z_{cx}(T, V, N)} \frac{\partial Z_{cx}(T, V, N)}{\partial N} = 0. \tag{11}$$

The corresponding equation of state is then

$$\tilde{\mu} - \frac{\partial F_{cx}(T, V, N)}{\partial N} = 0, \tag{12}$$

and we recover Eq. (9) through Eq. (6).

Note that the usual grand-canonical probability [Eq. (1)] must be rewritten, at coexistence, to include the presence of the interface area through the pseudochemical potential [Eq. (9)]. It is this coexistence grand-canonical probability [Eq. (10)] which displays the two-peaked distribution and not the usual grand-canonical probability, as proposed by Hill [17].

III. THERMOSTATISTICS OF PHASE COEXISTENCE FOR THE LATTICE GAS

In order to check our modified Hill's theory, we have carried out very careful simulations for the square lattice gas of L^2 lattice sites. For clearness, the latter model is briefly defined. Individual lattice sites may be empty or occupied by a single particle which interacts attractively with its nearest neighbors. The effective Hamiltonian in the grand-canonical ensemble may be written as

$$H = -\epsilon \sum_{i,j} \eta_i \eta_j + \mu \sum_i \eta_i, \tag{13}$$

with $\eta = 0(1)$ empty (occupied) sites. The fluid model can be easily mapped onto the magnetic Ising model, given by effective *Hamiltonian* $H = -J \sum_{i,j} \sigma_i \sigma_j + h \sum_i \sigma_i$, with $\sigma = +1(-1)$. The two models are equivalent if we make $J = 4\epsilon$ and $h = \mu + 2\epsilon$. In two dimensions, analytical results for the Ising model developed by Onsager are available [21] and serve as good test on the theory. The zero magnetic field condition for magnetic coexistence corresponds to a gas-liquid coexistence chemical potential $\mu_{cx}/\epsilon = -2$, and the reduced critical temperature is given by $t_C = k_B T_C/\epsilon \approx 0.57$.

So we must ask what are the implications of our proposal on the interpretation of simulation results. The answer is that some care must be taken with the interpretation of measured quantities. More specifically, the contribution of the interface behavior must be separated from bulk contributions.

In order to apply the thermostatistics of Sec. II to the lattice gas, we must study its properties in both the canonical and the grand-canonical ensembles.

In the first place, we obtain the $(T, V, \tilde{\mu})$ ensemble discrete probabilities $P(N; T, V, \tilde{\mu})$, given by Eq. (10), at different pseudochemical potentials $\tilde{\mu}$. Simulations are carried out via a combination of multicanonical [22,23] and Wang-Landau techniques [24], which allow us to look at events of very small probability.

In the Wang-Landau method, the density of states is estimated from a random walk in the space of the parameters one is interested in. Once a good estimate for the density of states is obtained, ensemble probabilities are trivially obtained. In our work, we have used the Wang-Landau's method [24] to estimate the density of states for energy and particle number. In the multicanonical technique [22,23], low-probability configurations are artificially privileged. The artificial effect is corrected before the averages are calculated. The combination of both techniques proved extremely successful in the estimation of density of states of very low probability, as we show in the following subsection.

The use of these techniques is central to our grand-canonical simulation results because they allow us to probe events of very low probability, between the gas and liquid densities. Below the reduced temperature $t_C \approx 0.57$, the probability densities present two maxima. By running the simulations for a large set of pseudochemical potentials, the three densities corresponding to the extrema of $P(N; T < T_c, V, \tilde{\mu})$ are used to construct the full $\tilde{\mu}$ vs $\langle \rho \rangle$ isotherms, in accordance with Eqs. (10)–(12).

Second, to test our corrected Hill's theory, Eq. (9) or (11), we have also run canonical ensemble simulations. Those were
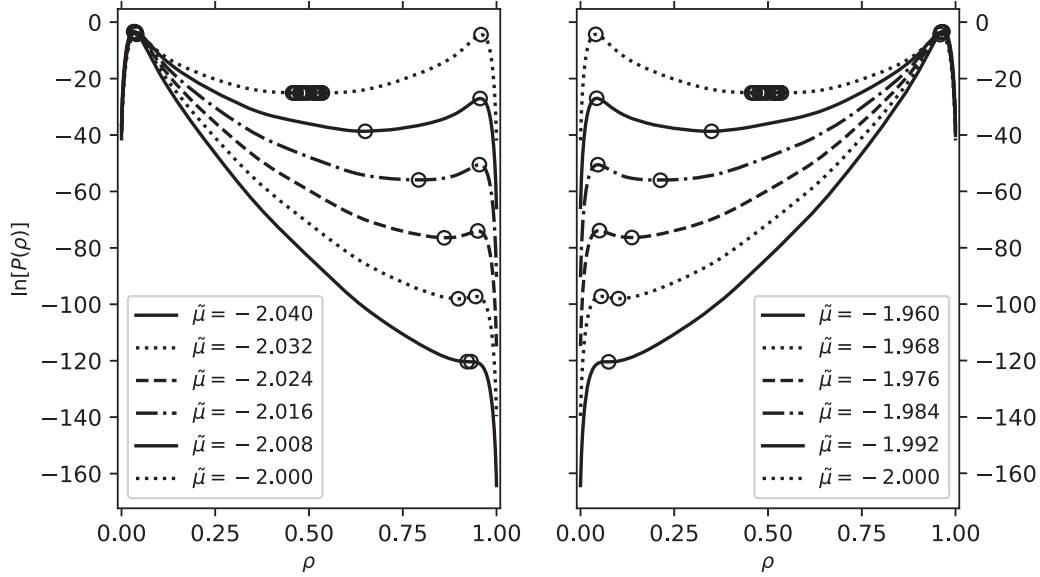
FIG. 2. Grand-canonical probabilities $P(N; \tilde{\mu})$. The left curve displays $P(N; \tilde{\mu})$ for decreasing values of the pseudochemical potential $\tilde{\mu}$ from coexistence and below, while the right curve displays $P(N; \tilde{\mu})$ for increasing pseudochemical potential values above coexistence. Circles indicate extrema of the distributions. Data are for $L = 40$ and temperature $t = 0.5$.

carried out through the usual Metropolis algorithm [25]. In this ensemble the numerical chemical potential is usually obtained through Widom's insertion method [20], which basically consists in calculating μ through the discretization of Eq. (3). Thus, the chemical potential μ may be shown to be a function of an average of the Boltzmann factor of the energy added to the system upon insertion of a "virtual" particle:

$$\mu(T, V, N) \equiv -k_B T \ln \frac{Z(T, V, N + 1)}{Z(T, V, N)}$$

$$= k_B T \ln \left[\frac{\rho}{\left\langle \exp\left(\frac{e_{\text{virtual–particle}}}{k_B T}\right)\right\rangle_{T,V,N}} \right]. \quad (14)$$

However, as we discussed above, Eq. (3), as well as its discretized version, Eq. (14), yield the chemical potential *only* for the case of homogeneous phases. Under conditions for coexistence, the system presents mostly configurations of phase separation with an interface. Thus, if the thermodynamic parameters correspond to coexistence conditions, the true chemical potential μ in simulations is no longer given by the discretized partial derivative of the canonical free energy. Rather, the latter is really a combination of the coexistence chemical potential and a term proportional to the gradient of the area of the interface, as given by Eq. (6). As a consequence, if the numerical experiment is carried out under coexistence conditions, Widom's insertion [Eq. (14)] yields a pseudochemical potential $\tilde{\mu}$ [Eq. (9)], and *not* the true chemical potential μ.

Note that, according to Eq. (9), $\tilde{\mu}$ must rise above the true coexistence chemical potential μ_{cx} if the area of the interface increases with particle number N, whereas the opposite is true if adding particles brings down the interface area. Also, if the interface area is maintained constant as particles are added to the system, the pseudochemical potential equals the true coexistence chemical potential, $\tilde{\mu} = \mu_{\text{cx}}$. This dependence on

the gradient of interface area with particle number is the origin of the loops, as we show in the following text.

Our procedure is as follows: (1) in the pseudo-grand-canonical ensemble $(T, V, \tilde{\mu})$, we measure the full discrete particle density probability distributions $P(N; \tilde{\mu})$, whose extrema yield a precise pseudochemical potential $\tilde{\mu}$ vs density $\langle \rho \rangle$ relations [Eqs. (10)–(11)]; (2) we obtain the pseudochemical potential isotherms $\langle \tilde{\mu} \rangle$ vs density ρ directly from usual *canonical* ensemble (T, V, N) simulations, through discretized Eq. (9) [see Eq. (14) and corresponding text]; and (3) results from the two different ensembles are compared. Simulations are carried out under periodic boundary conditions. As will be discussed later, this feature of simulations is essential in our proposal of data analysis.

Simulation results displayed in Figs. 1–5 are for lattice size $L = 40$. Figure 6 shows results for $L = 40, 50, 60, 70, 80$.

A. Simulation results: Comparison between canonical and grand-canonical ensembles and elimination of loops

The probabilities for the number of particles N in the system in the pseudo-grand-canonical ensemble [Eq. (10)] are represented in Fig. 2, for different values of the reduced pseudochemical potential $\tilde{\mu}/\epsilon$ [see Eq. (9)], at reduced temperature $t = k_B T/\epsilon$. It can be seen that the small density peak diminishes while the large density peak increases, for increasing $\tilde{\mu}/\epsilon$ up to $\tilde{\mu}/\epsilon = -2$. Above this value, the small density peak diminishes while the large density peak increases, as $\tilde{\mu}/\epsilon$ is continually augmented. For $\tilde{\mu}/\epsilon = -2$, one can see a small plateau at intermediate densities of the probability distribution, for which the small-density and high-density peaks are of the same height.

In the canonical (T, V, N) ensemble, of fixed density ρ, the usual Metropolis algorithm [25] was used to obtain $\langle \tilde{\mu} \rangle$, at each density, from the equation of state represented by Eq. (14).
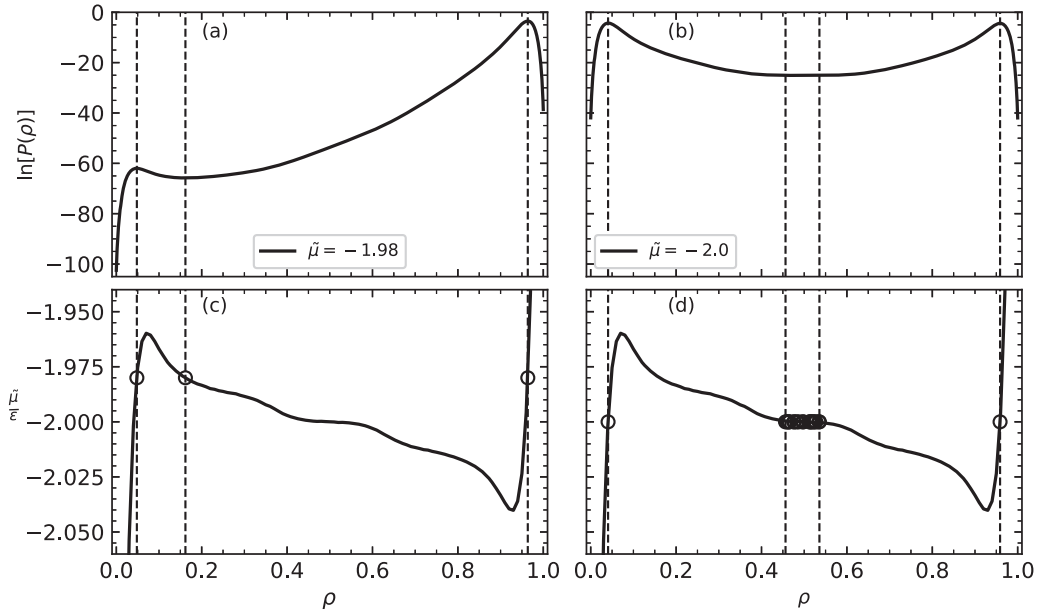
FIG. 3. Comparison between results obtained from (T, V, N) and $(T, V, \tilde{\mu})$ simulations. Panels (a) and (b) display distribution probability functions $P(N; T, V, \tilde{\mu})$ obtained in the grand-canonical ensemble for $\tilde{\mu} = -2.0$ and for $\tilde{\mu} = -1.98$, respectively. In panels (c) and (d), the continuous line represents the same pseudochemical potential isotherm, as obtained from canonical ensemble simulations. Circles indicate densities which correspond to extreme points of the grand-canonical $P(N; \tilde{\mu})$ (a, b) at fixed $\tilde{\mu} = -1.98$ (c) and at fixed $\tilde{\mu} = -2$ (d). For $\tilde{\mu} = -2.0$, the minima constitute a plateau. The dashed vertical lines serve to indicate the relation between the densities for the three extrema of $P(N; \tilde{\mu})$ with the corresponding densities on the pseudochemical potential $(T, V, \tilde{\mu})$ isotherms. Note the coincidence of $(\rho, \tilde{\mu})$ points obtained from simulations in the two different ensembles. Data points are for $L = 40$ and $t = 0.5$.

If the modified theory of Hill is fulfilled (even for finite systems), we expect the $(\rho, \tilde{\mu})$ values at the loops (Fig. 1) to be given by the extrema of the probabilities $P(N; \tilde{\mu})$ of the pseudo-grand-canonical ensemble (Fig. 2). Comparison between data obtained from runs in the two different ensembles is illustrated in Fig. 3. Figures 3(a) and 3(b) display grand-canonical probability distributions for two different pseudochemical potentials, $\tilde{\mu}/\epsilon = -1.98$ and $\tilde{\mu}/\epsilon = -2.0$. The densities corresponding to the extrema of the $P(N; \tilde{\mu})$ distributions are indicated by vertical dashed lines. They are also indicated by circles in Figs. 3(c) and 3(d) of the grand-canonical $\tilde{\mu}$ vs $\langle \rho \rangle$ isotherms. For $\tilde{\mu}/\epsilon = -1.98$, two maxima and a minimum can be seen. For $\tilde{\mu}/\epsilon = -2.0$, instead of a single minimum, one can see a plateau. Figures 3(c) and 3(d) represent $\langle \tilde{\mu} \rangle$ vs ρ isotherms (shown as continuous lines) obtained in the *canonical* ensemble from Widom's insertion. Note that the $(\langle \rho \rangle, \tilde{\mu})$ points obtained from the extrema of *grand-canonical* $P(N; \tilde{\mu})$, represented as circles in the lower plots, coincide with the $(\rho, \langle \tilde{\mu} \rangle)$ values measured in the canonical ensemble. This is true for $\tilde{\mu}/\epsilon = -1.98$, as well as for $\tilde{\mu}/\epsilon = -2.0$. For $\tilde{\mu}/\epsilon = -2.0$, the plateau in the pseudochemical potential $\tilde{\mu}$ coincides with the plateau (or continuous set of minima) of the $P(N; \tilde{\mu})$ probability distribution.

In Fig. 4 we compare the complete $t = 0.5$ isotherm $\tilde{\mu}(\rho)$ obtained from the numerical experiments in the two different ensembles through the procedure described for Fig. 3. It can be seen that results coincide entirely throughout the whole range of densities. The coincidence of both curves constitutes a good check on our modified version of Hill's theory.

Let us analyze the above results in light of state equation (6) [or Eq. (10)] and examine some of the consequences of this analysis.

Figure 3 shows that a small plateau for the canonical $\langle \tilde{\mu} \rangle$, seen at intermediate densities, is in correspondence with the continuous set of minima of the $P(N; \tilde{\mu})$ probabilities for N in the grand-canonical ensemble. According to Eq. (9), the presence of the plateau region in the canonical $\tilde{\mu}$ isotherms, at
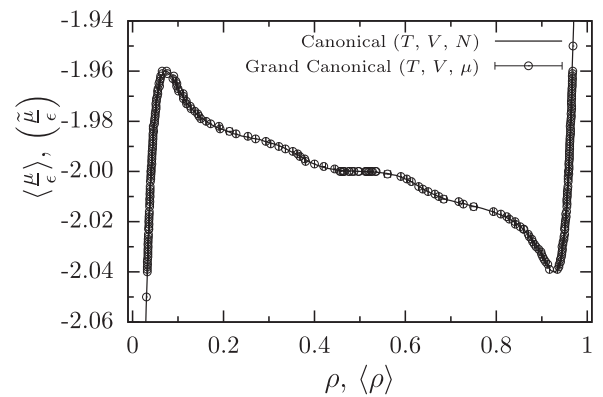

FIG. 4. Comparison between thermodynamics obtained from different ensembles. *Canonical ensemble*: $\tilde{\mu}$ is obtained directly from simulations through Eq. (14) at fixed density ρ. The corresponding canonical ensemble data are displayed as a continuous line. *Grand-canonical ensemble*: density ρ is obtained from extrema of the probability $P(N; T, V, \tilde{\mu})$ (see Fig. 3). The corresponding grand-canonical ensemble data are displayed as circles. $L = 40$ and $t = 0.5$.

intermediate densities, requires that interface area remains stationary under increase in particle number. Thus pseudo- and true chemical potential converge, which means that we can identify the coexistence potential with the plateau value, i.e., $\mu_{\mathrm{cx}}/\epsilon = \tilde{\mu}_{\mathrm{plateau}}/\epsilon = -2.0$. This hypothesis is confirmed by the grand-canonical probability distribution, which displays equal peaks for the same $\tilde{\mu}/\epsilon = -2.0$. It has long been known that the area beneath the two peaks must be equal at coexistence [26], [27], within an error which is exponentially small in L. For the lattice gas case, because of model symmetry, the two peaks are also of the same height. Therefore, both the canonical and the grand canonical data point to coexistence at $\tilde{\mu}/\epsilon = -2.0$. Note that this is also the value predicted by the exact Onsager theory.

The above discussion points to a second interesting result. It is tempting to extract the coexisting gas and liquid densities, ρ_{gas} and ρ_{liq}, from the intersection points of the extension of the canonical $\tilde{\mu} = -2.0$ plateau with the $\tilde{\mu}$ curve itself (see Fig. 1). This hypothesis is validated by the fact that the grand canonical distribution curve for $\tilde{\mu} = -2.0$ yields the same values for the densities corresponding to the maxima, that is, the same ρ_{gas} and ρ_{liq} predicted from the hypothesis on the canonical isotherm.

Now, how can we interpret the effects of variation in interface area upon the pseudochemical potential? Is there any additional information we can get from the corresponding loops?

Inspection of the isotherms of Fig. 3 shows that on the left side of the plateau, at lower densities, a "plus" half-loop is seen, with $\tilde{\mu}$ increasing above μ_{cx}. On the right side of the plateau, for larger densities, a "minus" half-loop is seen, with $\tilde{\mu}$ becoming lower than μ_{cx}. Equation (9) shows that the "plus" half-loop corresponds to $\frac{\partial A_{\mathrm{int}}}{\partial N} > 0$ and thus to increasing interface area with the addition of particles. Otherwise, as for the "minus" half-loop, it must occur under the condition of reduction of the interface area ($\frac{\partial A_{\mathrm{int}}}{\partial N} < 0$), with $\tilde{\mu}$ going below the coexistence potential, under addition of particles. Such behavior is compatible with the appearance of phase separation. As one goes over the lower density limit for coexistence, given by ρ_{gas}, the formation of a small dense bubble initiates, and an interface area appears and increases as particles are added, which causes the pseudopotential to rise above μ_{cx}. At intermediate densities, and under periodic boundary conditions, the interface stops increasing, and the pseudopotential equals the true coexistence potential. Above some density, the low-density phase begins shrinking, the interface area starts to contract, and the pseudopotential falls below the true chemical potential.

Rationalizing this result requires looking at the geometry of the interface, a procedure suggested in a few papers (see, for example, [7]). For the 2D system, the interface area is in fact a line, and the phase volume corresponds to a phase surface area. At small densities, the liquid phase constitutes a circle, with interface length given by $2\pi R$. Radius R increases with the addition of particles. At intermediate densities, and under periodic boundary conditions, the circle deforms towards a stripe of length L. For the stripe, interface length is given by $2L$ and is constant while particle number and stripe width increase. For larger densities, the liquid phase tends to occupy the whole lattice, and the gas phase shrinks to a
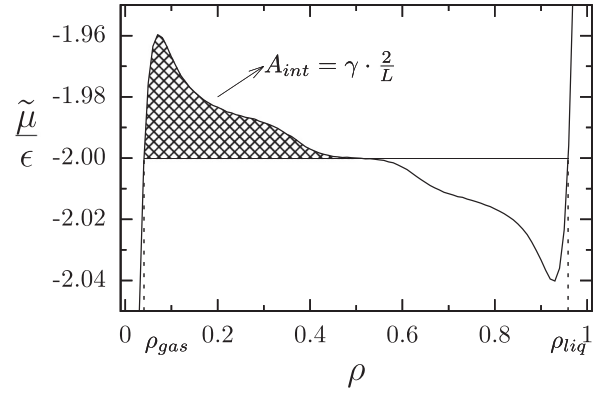

FIG. 5. True vs pseudochemical potential isotherms. Extension of the plateau in $\tilde{\mu}(\rho)$ (thin line) identifies limits of coexistence and gas and liquid densities ρ. The thick line represents the true chemical potential isotherm $\mu(\rho)$. Integration of the $\tilde{\mu}$ "plus" loop allows for calculation of surface tension $\gamma(t)$. Data are for $L = 40$ and $t = 0.5$.

circle. The interface length A_{int} decreases, as circle radius R diminishes. Minimizing the free energy of the interface, $F_{\mathrm{int}} = \gamma(t)A_{\mathrm{int}}$ implies minimizing interface area. This implies that one of the phases will present a circular form for $0 < R < L/\pi$ and tend to a stripe for R outside this range. Similar reasoning for a 3D system yields the condition $0 < R < L/\pi$ for a spherical phase which deforms into a rectangular box otherwise. In the stripe (rectangular box, in $d = 3$) region, A_{int} is constant, in spite of the increase in particle number, and thus pseudochemical potential $\tilde{\mu}$ remains constant and equal to μ_{cx}, from Eq. (9). The evolution of geometry of phase coexistence with global density is illustrated through the presentation of a few configurations as insertions in Fig. 1.

The reasoning presented above allows us to obtain the true coexistence chemical potential, as well as the coexistence densities ρ_{gas} and ρ_{liq}. Figure 5 displays true and pseudochemical potentials. The effect of interface area on the isotherms is subtracted, and true μ vs density isotherms are obtained.

The true coexistence chemical potential μ_{cx} presents *no* thermodynamic instabilities and is in accordance with the convexity essential properties of thermodynamic potentials. This is our principal result. Correct treatment of interface thermodynamics removes instability and yields plateaus instead of loops.

B. Surface tension

An important check on our proposal is possible. In the case of the 2D lattice gas, an analytic expression for the interface tension was presented in Onsager's paper [21], which, for the lattice interacting gas, is given by

$$\frac{\gamma(t)}{\epsilon} = \frac{1}{2} - t \ln\left[\frac{1 + e^{-\frac{1}{2t}}}{1 - e^{-\frac{1}{2t}}}\right], \qquad (15)$$

with $t \equiv k_B T/\epsilon$.

Usually [5,6,28] surface tension is calculated from the pseudo-grand-canonical probability distribution function $P(N; \tilde{\mu})$ at coexistence. In our proposal, numerical results for the function $\tilde{\mu}$ obtained in the canonical ensemble allow direct
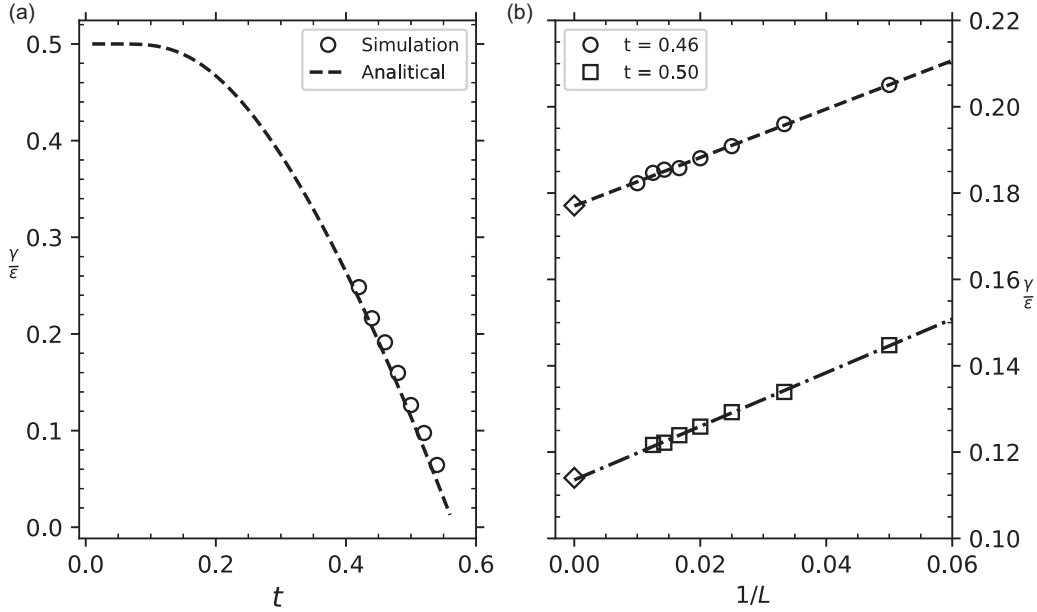
FIG. 6. Lattice gas surface tension $\gamma(t)$. In the left figure our $L = 40$ data for $\gamma(t)$ are displayed as circles and can be compared to Onsager's exact result, Eq. (15) (dashed line). The right figure displays behavior with size L for temperatures $t = 0.45$ and $t = 0.5$. The exact results, corresponding to $L \to \infty$, are indicated with the diamond symbol. For $t = 0.46$, fitting yields $\gamma(t, L \to \infty) = 0.1135$, compared to exact $\gamma(t = 0.46) = 0.1140$. For $t = 0.5$, fitting yields $\gamma(t, L \to \infty) = 0.1770$, compared to exact $\gamma(t = 0.5) = 0.1771$.

calculation of surface tension γ from the pseudochemical potential $\tilde{\mu}$ isotherms.

This can be done through the integration of Eq. (9), in the region of one of the semiloops, on either side of the plateau.

The rationale is as follows: (1) The variation of $\tilde{\mu}$ with density ρ, at fixed temperature, is a function solely of the variation in the interface area between the coexisting phases, since the interface tension γ is a function only of temperature [see Eq. (5)]. (2) The interface has zero area up to the gas density ρ_{gas} and rises rapidly beyond ρ_{gas}, as density is increased, reaching some maximum rate, after which rate decreases and at some density becomes null, initiating the plateau region for a set of densities which we denote as ρ_{plateau}. (3) The area of the flat interface $A_{\text{flat}-\text{int}}(T, L)$ remains constant in the plateau region of the pseudochemical potential $\tilde{\mu}$ (see discussion in Sec. A above).

Reasoning in (1)–(3) allows us to contract Eqs. (5) and (9), and write

$$\gamma(t; L) = \frac{V(L)}{A_{flat-int}(L)} \int_{\rho_{\text{gas}}(t)}^{\rho_{\text{plateau}}} [\tilde{\mu}(t) - \mu_{\text{cx}}(t)] \, d\left(\frac{N}{V}\right). \quad (16)$$

Equation (16) is a general result and can be used for calculating interface surface tension $\gamma(t)$ for any system which presents "loops" in the pseudochemical potential and a plateau. "Loops" must be integrated numerically, and interface area must be measured.

For squares or cubes, and under periodic boundary conditions, at temperatures at which roughness of the interface may be neglected, we may write $A_{flat-int}(L) = 2L^{d-1}$ [with $A_{flat-int}(L) = 2L$, a lateral perimeter, for $d = 2$, or $A_{flat-int}(L) = 2L^2$, a set of lateral surfaces, for $d = 3$].

We thus have for the interface tension $\gamma(t; L)$

$$\gamma(t; L) = \frac{L}{2} \int_{\rho_{\text{gas}}(t)}^{\rho_{\text{plateau}}} [\tilde{\mu} - \mu_{\text{cx}}]_t \, d\rho \quad (17)$$

since $V = L^d$. This is a general result for systems of cubic symmetry, and independent of dimensionality d. Figure 5 illustrates our procedure for the 2D lattice gas.

Figure 6(a) shows our numerical results for surface tension $\gamma(t; L)/\epsilon$ for different temperatures, as compared to the analytical prediction by Onsager [21]. In Fig. 6(b) it can be seen that $\gamma(L)$ decreases linearly with $1/L$ and that extrapolation to infinite L yields Onsager's results, within an error of less than 0.5%. Therefore one may write

$$\gamma(t; L) = \gamma(t; L \to \infty) + o(1/L), \quad (18)$$

which implies that the numerical area under the loop must scale as $1/L$ [Eq. (17)]. So the loops should disappear as $L \to \infty$, which explains their slow elimination described by other authors (see, for example, [6]).

IV. CONCLUSION

In this study we have found an interpretation for the forbidden loops in the chemical potential isotherms usually encountered for systems at coexistence in numerical simulations in the canonical ensemble [4–7]. We have shown that proper thermodynamic analysis of the coexistence free energy, F_{cx}, which must include the interface contribution, $F_{\text{cx}} = F_{\text{bulk}} + F_{\text{int}}$, implies an important modification of the usual textbook equation of state for the chemical potential. The usual partial derivative of the free energy with respect to particle number, $\left(\frac{\partial F_{\text{cx}}}{\partial N}\right)_{T,V}$, does *not* yield the true chemical potential. We have called the average quantity measured a pseudochemical potential, which is equal to the sum of the

true coexistence chemical potential and a term which comes from the interface energy, and is proportional to the gradient of the interface area. We show that it is this additional term which produces the loops displayed by the pseudopotential. Loops disappear for the true chemical potential.

In numerical experiments in the canonical ensemble, the chemical potential is usually obtained from Widom's insertion method, derived from discretization of the usual textbook equation of state. Under phase separation, such a procedure yields the pseudopotential. In order to obtain the true chemical potential, a hypothetical alternative would be to take configurations of constant interface area, i.e., to look for $(\frac{\partial F_{cx}}{\partial N})_{T,V,A_{int}}$. This is unfeasible in simulations. However, in the framework of our proposal, investigation of the "pseudo"-chemical potential isotherms may yield rich information on phase separation.

We have undertaken such an investigation for the case of phase coexistence in the square lattice gas. We show the following: (1) the true coexistence chemical potential may be obtained from the small plateau displayed by the pseudochemical potential isotherms at intermediate densities; (2) the coexisting densities may be extracted from the crossing of the extension of the plateau and the pseudopotential isotherm; and (3) the interface tension may be measured from the integration of $\tilde{\mu} - \mu_{cx}$ along one of the semiloops. The surface tension of the 2D lattice gas was measured as described in (3) and converges, for large L, to the exact value obtained analytically by Onsager in the 1940s.

The justification for our proposal in the last paragraph comes from the adaptation of Hill's theory, with the introduction of the interface free energy into his arguments. A test of the adapted theory was undertaken, by comparing data for the pseudochemical potential coming from the grand canonical to those coming from the canonical ensemble. In the first case, data for the isotherms at a given pseudochemical potential are taken from the extrema of the probability distribution. In the second case, the pseudochemical potential is measured from Widom's insertion procedure. We show entire compatibility of the two sets of data. Regions of stationarity of the probability distribution are directly related to the $\tilde{\mu}$ plateau regions and to constant interface area. The latter justifies taking the plateau as the true coexistence potential μ_{cx}.

In summary, we have shown that no violation of the second law of thermodynamics really takes place, and that proper convexity of the chemical potential is recovered, if it is correctly calculated, by subtracting the effect of the variation in interface area. As a side product of our analysis, we propose a much simpler method for the calculation of surface tension, directly from the canonical pseudopotential isotherms, turning unnecessary the nontrivial calculation of the full grand-canonical distribution probability function.

We have presented very good results for the well-known lattice gas model, which, we believe, is a good test of our ideas. There are no restrictions, however, to the application of the procedure to other lattice or off-lattice fluid models.

[1] T. Andrews, The Bakerian Lecture: On the continuity of the gaseous and liquid states of matter, Philos. Trans. R. Soc. London **159**, 575 (1869).

[2] J. Van der Waals, Over de continuiteit van den gas-en vloeistoftoestand (On the continuity of the gas and liquid state), Ph.D. thesis, University of Leiden, 1873.

[3] K. Huang, *Statistical Mechanics* (Wiley, New York, 1987).

[4] H. Furukawa and K. Binder, Two-phase equilibria and nucleation barriers near a critical point, Phys. Rev. A **26**, 556 (1982).

[5] K. Binder, Monte Carlo calculation of the surface tension for two- and three-dimensional lattice-gas models, Phys. Rev. A **25**, 1699 (1982).

[6] M. Schrader, P. Virnau, and K. Binder, Simulation of vapor-liquid coexistence in finite volumes: A method to compute the surface free energy of droplets, Phys. Rev. E **79**, 061104 (2009).

[7] K. Binder, B. J. Block, P. Virnau, and A. Tröster, Beyond the van der Waals loop: What can be learned from simulating Lennard-Jones fluids inside the region of phase coexistence, Am. J. Phys. **80**, 1099 (2012).

[8] S. Schnabel, D. T. Seaton, D. P. Landau, and M. Bachmann, Microcanonical entropy inflection points: Key to systematic understanding of transitions in finite systems, Phys. Rev. E **84**, 011127 (2011).

[9] D. H. E. Gross, *Microcanonical Thermodynamics* (World Scientific, Singapore, 2001).

[10] H. B. Callen, *Thermodynamics and an Introduction to Thermostatics*, 2nd ed. (Wiley, New York, 1985).

[11] R. K. Pathria and P. D. Beale, *Statistical Mechanics*, 3rd ed. (Academic Press, Boston, 2011).

[12] L. Landau and E. Lifchitz, *Physique Statistique*, 3rd ed. (Mir, Moscow, 1984).

[13] M. J. d. Oliveira, *Termodinâmica* (Livraria da Física, São Paulo, Brazil, 2005).

[14] S. Prestipino and P. V. Giaquinta, The concavity of entropy and extremum principles in thermodynamics, J. Stat. Phys. **111**, 479 (2003).

[15] R. B. Griffiths and J. C. Wheeler, Critical points in multicomponent systems, Phys. Rev. A **2**, 1047 (1970).

[16] B. J. Block, S. K. Das, M. Oettel, P. Virnau, and K. Binder, Curvature dependence of surface free energy of liquid drops and bubbles: A simulation study, J. Chem. Phys. **133**, 154702 (2010).

[17] T. L. Hill, *Statistical Mechanics: Principles and Selected Applications* (Dover, 1987).

[18] D. P. Landau, Monte Carlo studies of finite size effects at first and second order phase transitions, in *Finite Size Scaling and Numerical Simulation of Statistical Systems*, edited by V. Privman (World Scientific, Singapore, 1990), pp. 223–260.

[19] J. S. Rowlinson and B. Widom, *Molecular Theory of Capillarity* (Oxford University Press, Oxford, 1982).

[20] B. Widom, Some topics in the theory of fluids, J. Chem. Phys. **39**, 2808 (1963).

[21] L. Onsager, Crystal statistics. I. A two-dimensional model with an order-disorder transition, Phys. Rev. **65**, 117 (1944).

[22] B. A. Berg and T. Neuhaus, Multicanonical algorithms for first order phase transitions, Phys. Lett. B **267**, 249 (1991).

[23] B. A. Berg and T. Neuhaus, Multicanonical ensemble: A new approach to simulate first-order phase transitions, Phys. Rev. Lett. **68**, 9 (1992).

[24] F. Wang and D. P. Landau, Efficient, multiple-range random walk algorithm to calculate the density of states, Phys. Rev. Lett. **86**, 2050 (2001).

[25] N. Metropolis, A. W. Rosenbluth, M. N. Rosenbluth, A. H. Teller, and E. Teller, Equation of state calcula-

tions by fast computing machines, J. Chem. Phys. **21**, 1087 (1953).

[26] K. Binder and D. P. Landau, Finite-size scaling at first-order phase transitions, Phys. Rev. B **30**, 1477 (1984).

[27] C. Borgs and R. Kotecky, A rigorous theory of finite-size scaling at first-order phase transitions, J. Stat. Phys. **61**, 79 (1990).

[28] A. Tröster, M. Oettel, B. Block, P. Virnau, and K. Binder, Numerical approaches to determine the interface tension of curved interfaces from free energy calculations, J. Chem. Phys. **136**, 064709 (2012).